Journal of CO_2 Utilization 29 (2019) 117–125

Contents lists available at ScienceDirect

Journal of CO_2 Utilization

journal homepage: www.elsevier.com/locate/jcou

Production of precipitated calcium carbonate particles from gypsum waste using venturi tubes as a carbonation zone

Mahmut Altiner[a,*], Soner Top[a,b], Burçin Kaymakoğlu[c], İsmail Yiğit Seçkin[d], Hüseyin Vapur[a]

[a] Department of Mining Engineering, Çukurova University, Adana, 01330, Turkey
[b] Department of Material Science and Nanotechnology, Abdullah Gul University, Kayseri, 38080, Turkey
[c] Department of Materials Engineering, Adana Science and Technology University, Adana, 01250, Turkey
[d] Department of Environmental Engineering, Çukurova University, Adana, 01330, Turkey

ARTICLE INFO

Keywords:
Mineral carbonation
Desulfurization gypsum
Precipitated calcium carbonate
Venturi tube
Calcite crystals

ABSTRACT

In this study, we investigated the production of precipitated calcium carbonate (PCC) particles from desulfurization gypsum (DG) waste using a new experimental apparatus that is divided into two main parts: carbonation and stabilization zones. The solution was circulated via a pump from the stabilization zone to the carbonation zone where different types of Venturi tube were used for the reaction of CO_2 with solution to produce PCC particles. The effects of CO_2 flow rate, circulation rate, and Venturi types on the properties of the produced PCC particles were studied using X-ray diffraction (XRD), scanning electron microscopy (SEM), and particle size analyses. The conductivity and pH values of the solution were monitored during the carbonation. In addition, the reactivity of selected PCC was determined to evaluate its use as a sorbent in a desulfurization unit. The experimental results indicate that the Venturi tube had a strong effect on the reaction time and properties of PCC particles. The use of a Venturi tube resulted in a decrease in the time required for producing PCC particles, which were smooth, well-crystallized, and nano-sized cubic crystals. However, when no Venturi tube was used, hollow spherical crystals formed along with cubic crystals. It was found that the reactivity of selected PCC particles produced using Venturi tube was rather higher ($52 \times 10^{-4}\,min^{-1}$), indicating that the PCC can be used as a sorbent in the desulfurization unit.

1. Introduction

Three types of gypsum wastes, desulfurization gypsum (DG), phosphogypsum (PG), and red gypsum (RG), are generated from different industrial applications. While DG is generated from a power station, PG and RG are respectively generated from phosphoric acid production [1] and ilmenite ore processing to obtain TiO_2 particles [2]. DG is produced through a reaction between the sulfur gas and lime or limestone sorbents in a desulfurization unit where sulfur gas is captured as an inorganic material in a power station. DG and PG wastes mainly consist of CaO, SO_3, and H_2O, as well as small impurities (Fe_2O_3, SiO_2, and Al_2O_3), making them useful in many industrial areas such as chemistry (as an adsorbent for removing fluoride [3] or phosphorus [4]), agriculture (as a soil amendment [5]), construction (wallboard or fire-resistant panel manufacturing [6], prefabricated building material [7], and sulfoaluminate cement [8,9]).

Moreover, the gypsum wastes all have a good potential to be evaluated for CO_2 capture because they contain high Ca content. Many recent studies [10–27] have been investigated to determine the potential of GW to capture CO_2 via mineral carbonation, which is one of the carbon capture and storage technologies. This method is based on a reaction between CO_2 and an alkaline metal (such as Mg or Ca) to produce stable inorganic carbonate materials using a one-step or two-step mineral carbonation process. Calcite, aragonite, and vaterite crystals are the polymorphs of $CaCO_3$ particles, which can be prepared using different production conditions. Vaterite crystals have been obtained using the one-step carbonation, and when the two-step carbonation was performed according to Song et al. [10], all particles were formed as calcite crystals. In a follow-up study [16], due to an increase in the amount of ammonia, vaterite became the major phase in produced $CaCO_3$ particles; the aragonite and vaterite crystals were observed by scanning electron microscopy (SEM) and X-ray diffraction (XRD) analyses, respectively, in the presence of ethanol in water under excess ammonia conditions. Furthermore, calcite with twinned pseudo-spherical crystals have been prepared in the presence of polyacrylic acid using the one-step process [20].

* Corresponding author.
E-mail address: maltiner@cu.edu.tr (M. Altiner).

https://doi.org/10.1016/j.jcou.2018.12.004
Received 19 October 2018; Received in revised form 22 November 2018; Accepted 7 December 2018
Available online 11 December 2018

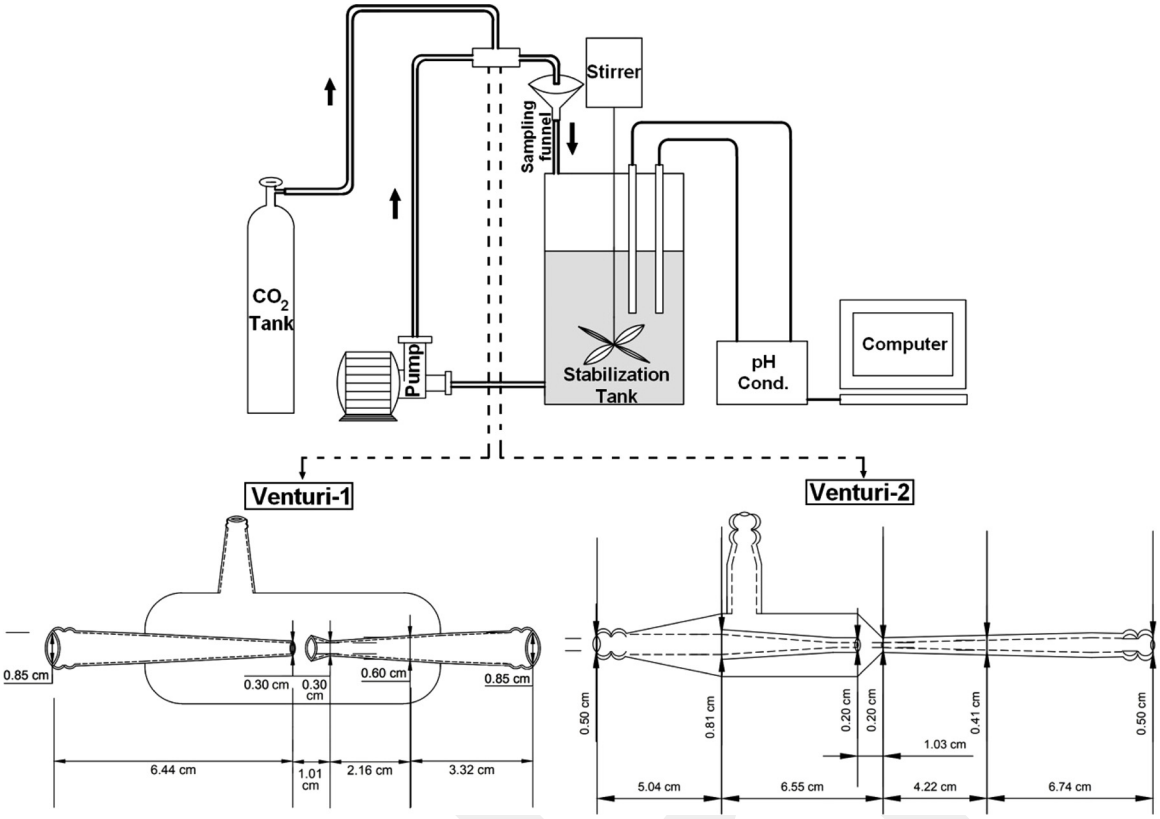

Fig. 1. Experimental apparatus used in this study (not scaled) and technical drawing of Venturi tubes.

Both NH_4OH and NaOH have been used as an extracting agent to promote DG carbonation. The effects of these extracting agents on the properties of $CaCO_3$ particles have been investigated by previous researchers [15,28]. They observed untransformed DG particles together with a mixture of vaterite or calcite crystals in the presence of NH_4OH, whereas when NaOH was used as an extracting agent, all produced particles showed sharp peaks in an XRD graph corresponding to the calcite crystals. Furthermore, reaction temperature and CO_2 flow rate had strong influences on the conversion of DG to nano-sized $CaCO_3$ particles using the one-step process conducted at a temperature of 40 °C with CO_2 flow rate of 0.138 l/min [18].

In a simulated thermodynamic model to understand the transformation of DG to $CaCO_3$ particles using the one-step process [14], the effect of solid-to-liquid ratio on the carbonation was negligible and $CaCO_3$ particles could be produced with a high conversion rate (> 99%) using the following conditions: ammonia-to-DG molar ratio of > 2.5 and CO_2-to-DG molar ratio of > 1 at ambient temperature. Moreover, an increase in reaction temperature resulted in a decrease in the absorption property of CO_2, indicating that a longer reaction time is needed for $CaCO_3$ production from DG. In addition to the conversion of RG to calcite crystals at ambient temperature [25], synthetic siderite (FeC_3) particles can be obtained from the RG using the two-step process [29], but specific conditions such as high CO_2 pressure (10 bar) and reaction temperature (150 °C) are required.

In the literature, different reactors such as high-pressure jet homogenizer [30], mixed flow reactor [31], draft-tube reactor [32], and jet flow reactor [33] have been used to produce $CaCO_3$ particles. Previous studies have revealed that compared to the traditional batch reactor, these reactors have superior advantages due to a higher reproducibility of $CaCO_3$ with desired qualities under controlled chemical conditions [31].

In this study the reaction of Ca^{2+} ions with CO_2 gas to produce precipitated calcium carbonate (PCC, $CaCO_3$) particles was carried out in a Venturi tube, rather than the abovementioned reactors; this does not only provide a turbulence flow but creates pico-nano CO_2 bubbles during the carbonation. In particular, the Venturi tube has been used to improve the interaction between air bubbles and fine particles in a flotation process [34]. To the best of our knowledge, this is the first time that Venturi tube was used as a carbonation zone and PCC particles were formed. In the present study, the effects of Venturi tube type, CO_2 flow rate, and circulation rate on the reaction time and properties of PCC particles were investigated in detail using XRD, SEM, and particle size distribution analyses. The conductivity and pH values of the solution were monitored during the carbonation. Control experiments were performed without using any Venturi tube. The reactivity of the selected PCC particles was further determined using a pH-stat method, and the results were compared with those of previous studies.

2. Experimental procedure

2.1. Materials

The DG sample used in this study was collected from a power station in Adana/Turkey. The chemical composition of DG is as follows: 46.51% SO_3, 32.50% CaO, 19.70% H_2O, and 1.29% impurities (Al_2O_3, MnO, and Fe_2O_3). CO_2 gas with a high purity (99.99%) was purchased from Cangaz, Adana. Pure water (conductivity: 0.06 ± 0.01 μS/cm) was used in each experiment. NaOH was of analytical grade and used without any further purification.

2.2. Preparation of precipitated calcium carbonate crystals from desulfurization gypsum

Before the carbonation, DG was converted into calcium hydroxide $Ca(OH)_2$ under the following experimental conditions: 12 mol of DG, 2.1 M ratio of $[OH]^-/Ca^{2+}$ ($NaOH$ was used as an OH^- source), 1:13 of solid-to-liquid ratio (g:mL), 300 rpm of stirring speed at a temperature of 20 °C for 1 h [28]. After the conversion process, a solid/liquid

separation was performed to collect the produced $Ca(OH)_2$ particles. The experimental apparatus used in this study can be seen in Fig. 1. It comprises seven parts: a $Ca(OH)_2$ solution tank, Teflon-coated mechanical stirrer, pump for liquid circulation, Venturi tube for mixing solution and CO_2, CO_2 tube, CO_2 flow meter, and data logger to monitor pH and conductivity values of the solution in the tank. The solution leaves from the bottom of the stabilization tank and goes into the Venturi tube via the pump, which can be adjusted to different circulation rates. The CO_2 was then bubbled into the Venturi tube, in which Ca^{2+} ions react with CO_2 to produce PCC particles. Therefore, the solution tank is classified as a stabilization zone, while the Venturi tube is a carbonation zone.

Each Venturi tube provides turbulence flows during the carbonation. The Reynolds number of the solution is determined using the following equation.

$$\mathrm{Re} = \frac{u \times D}{x} \quad (1)$$

Here, R_e is the Reynolds number, u is the circulation rate of the solution (m/s), D is the internal diameter of the Venturi (m), and x is the kinematic viscosity of the solution (1.0034×10^{-6} mm^2/s at 20 °C).

The Reynolds number of the solution in the Venturi-1 (V1) was varied between 20.50×10^4–116×10^4 in the carbonation zone, while the Reynolds number of the solution was in a range 35×10^4–18.58×10^6 in the Venturi-2 (V2) as its internal diameters were smaller than those of the V1. The concentration of $Ca(OH)_2$ in the solution of 12 l was 15 mM. The solution was stirred at 500 rpm. The effects of CO_2 flow rate, circulation rate, and Venturi type on the production of PCC from DG were investigated in detail. The conductivity and pH values of the solution were monitored using an equipment (Gondo, PL-700AL) during the carbonation. The CO_2 flow was turned off to complete the carbonation when the conductivity of the solution decreased almost to zero. Table 1 lists the experimental conditions in this study. These are denoted as CFx-Rx-Vx. For example, the notation CF1-R1-V1 indicates that the experiment was performed under CO_2 flow rate of 1 l/min, circulation rate of 32.32 m/s, and Venturi-1. For comparison, control experiments were performed at the same conditions without circulating the solution, and the notation VX indicates control experiment with no Venturi tube.

2.3. Characterization test

The phase properties of the PCC were identified using a Rigaku XRD equipped with Cu Ka radiation in the 2ø range of 15°–85° with a 0.02 step size, and the patterns were evaluated using a PDXL software for mineral identification. Debye-Scherrer equation [35] were also used to determine the crystallite size of PCC. The surface morphologies of selected PCC were further imaged by a SEM, Quanta FEG 650). The particle size distribution of the PCC determined using a Malvern Mastersizer (300 U) was evaluated based on the SPAN factor, which was calculated using the following equation.

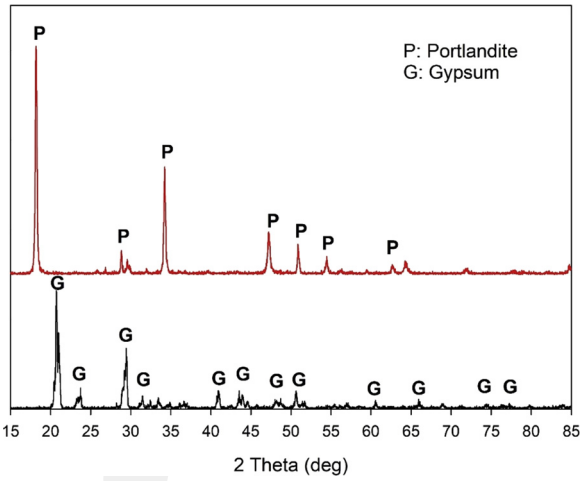

Fig. 2. XRD patterns showing the conversion of desulfurization gypsum (DG) to calcium hydroxide [$Ca(OH)_2$] particles.

$$SPAN = \frac{d_{90} - d_{10}}{d_{50}} \quad (2)$$

where d_{90}, d_{50}, and d_{10} values are particle sizes indicating 90%, 50%, and 10% of the cumulative undersize distribution curve belonging to the produced PCC, respectively.

2.4. Reactivity test

The experimental method used for determining the dissolution rate of the PCC particles has been explained in previous studies [36–38]. This procedure stimulates the conversion of sulfur gas to gypsum waste in a wet flue gas desulphurization system. In the present study, 1 g of selected PCC particles was dissolved in 0.625 dm^3 of pure water that had been stirred at 500 rpm. During the reactivity test, pH of the solution was fixed at 5 by the addition of 0.1 HCl. The amount of consumed acid volume varying time was measured to determine the

Table 1
Experimental conditions for producing PCC from DG.

Experiment Code	CO_2 (l/min)	Circulation rate						Venturi Type
		From the solution tank to the Venturi		Inlet of Venturi		Carbonation zone in Venturi		
		Velocity (m/s) *	Re*	Velocity (m/s) *	Re*	Velocity (m/s) *	Re*	
CF1-R1-V1	1	32.32	20.50×10^4	32.32	20.50×10^4	58.09	41×10^4	V1
CF0.5-R1-V1	0.5	32.32	20.50×10^4	32.32	20.50×10^4	58.09	41×10^4	V1
CF0.3-R1-V1	0.3	32.32	20.50×10^4	32.32	20.50×10^4	58.09	41×10^4	V1
CF1-R2-V1	1	64.64	58.09×10^4	64.64	58.09×10^4	518.96	116×10^4	V1
CF0.5-R2-V1	0.5	64.64	58.09×10^4	64.64	58.09×10^4	518.96	116×10^4	V1
CF0.3-R2-V1	0.3	64.64	58.09×10^4	64.64	58.09×10^4	518.96	116×10^4	V1
CF1-R1-V2	1	32.32	20.50×10^4	93.77	34.98×10^4	583.83	929×10^4	V2
CF0.5-R1-V2	0.5	32.32	20.50×10^4	93.77	34.98×10^4	583.83	929×10^4	V2
CF0.3-R1-V2	0.3	32.32	20.50×10^4	93.77	34.98×10^4	583.83	929×10^4	V2
CF1-R2-V2	1	64.64	58.09×10^4	187.54	69.96×10^4	1167.63	18.58×10^6	V2
CF0.5-R2-V2	0.5	64.64	58.09×10^4	187.54	69.96×10^4	1167.63	18.58×10^6	V2
CF0.3-R2-V2	0.3	64.64	58.09×10^4	187.54	69.96×10^4	1167.63	18.58×10^6	V2
CF1-RX-VX	1	X						VX
CF0.5-RX-VX	0.5	X						VX
CF0.3-RX-VX	0.3	X						VX

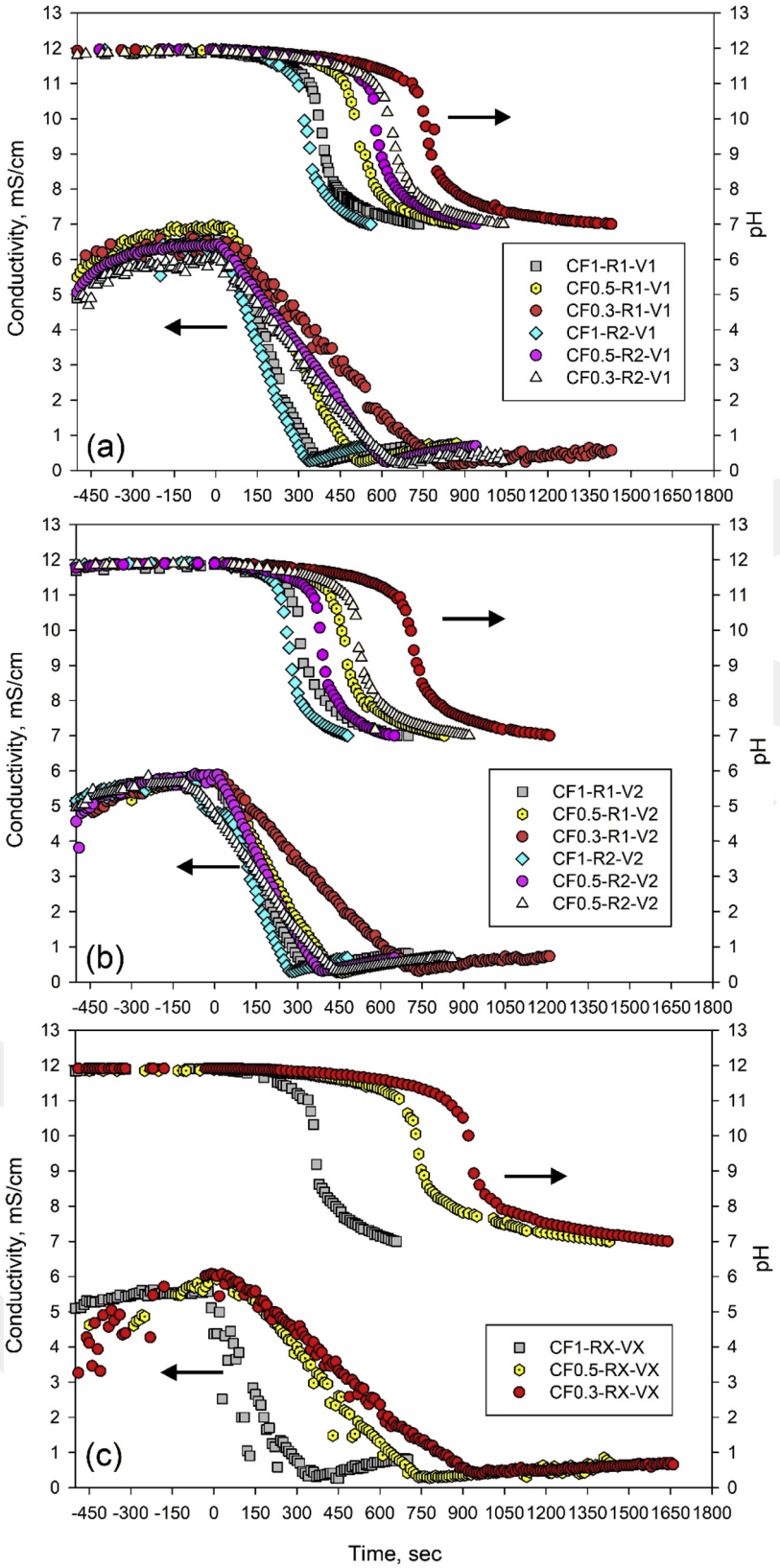

Fig. 3. Change in pH and conductivity values of the solution using (a) V1, (b) V2, and (c) VX.

conversion ratio of PCC particles. The dissolution rate of PCC particles was then calculated. Afterward, the reaction rate constant was determined using the following equation, according to the shrinking core model.

$$1 - (1 - X)^{\frac{1}{3}} = kt \tag{3}$$

where X is the conversion of the PCC particles, t is time (min), and k is the overall reaction constant (min^{-1}).

Table 2
Precipitation rate (PR) of PCC and required reaction time at different production conditions.

Exp. Code	PR (μM/s)	Reaction Time (s)	Exp. Code	PR (μM/s)	Reaction Time (s)	Exp. Code	PR (μM/s)	Reaction Time (s)
CF1-R1-V1	30.77	390	CF1-R1-V2	31.58	380	CF1-RX-VX	32.43	370
CF0.5-R1-V1	23.08	520	CF0.5-R1-V2	26.09	460	CF0.5-RX-VX	15.38	780
CF0.3-R1-V1	14.81	810	CF0.3-R1-V2	16.22	740	CF0.3-RX-VX	12.37	970
CF1-R2-V1	36.36	330	CF1-R2-V2	42.86	280			
CF0.5-R2-V1	19.35	620	CF0.5-R2-V2	30.77	390			
CF0.3-R2-V1	18.18	660	CF0.3-R2-V2	26.67	450			

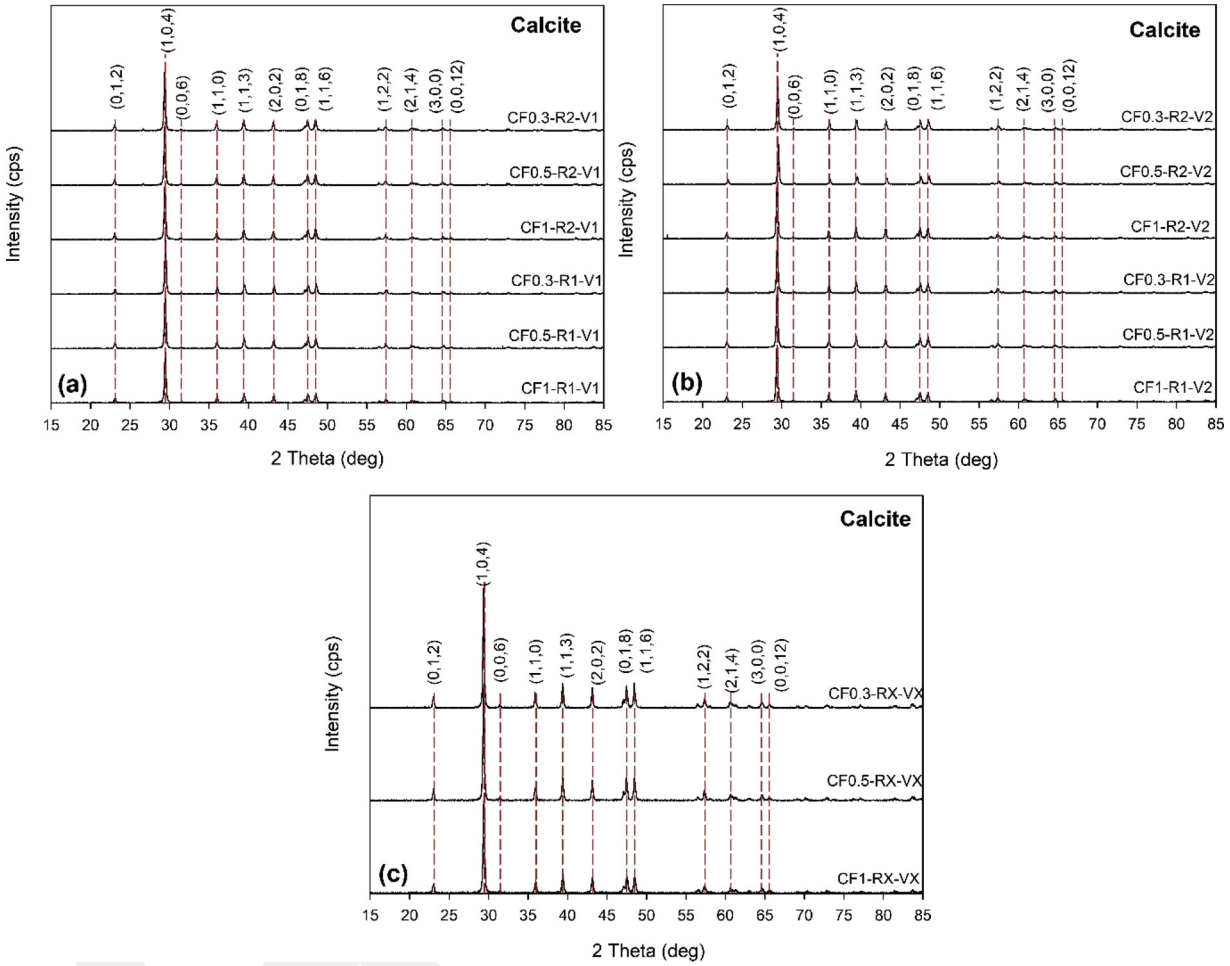

Fig. 4. XRD patterns of produced PCC particles using (a) V1, (b) V2, and (c) VX.

3. Results and discussion

3.1. Preparation of $Ca(OH)_2$ particles from DG

First, alkali leaching of DG was conducted under the above-mentioned conditions to produce $Ca(OH)_2$ particles. The XRD analysis results (Fig. 2) revealed that the conversion of DG to $Ca(OH)_2$ particles, which were identified as a portlandite mineral, was performed successfully. The major peaks were identified at $2\theta = 18.19^\circ$, 28.79°, 34.23°, 47.22°, 50.89°, 54.49°, and 62.61°. This finding is in good agreement with those of a previous study [26].

Thereafter, the obtained $Ca(OH)_2$ particles were dissolved in 12 l pure water, and the solution concentration was kept as 15 mM, which is lower than that of the solubility limit of $Ca(OH)_2$ [39]. Before CO_2 was bubbled in the solution, the solution was stirred for 450 s to dissolve all $Ca(OH)_2$ particles as Ca^{2+} and OH^- ions according to the chemical equilibrium equation given in a previous study [40]. The pH and conductivity of the solution were measured as 12 ± 0.01 and 6 ± 0.01 mS/cm, respectively. Subsequently, CO_2 with different flow rates was bubbled into the carbonation zone (Venturi tube) where the solution and CO_2 were mixed. Then the pump was started to circulate the solution from the stabilization zone (solution tank) to the carbonation zone.

3.2. Production of precipitated calcium carbonate crystals

Fig. 3 shows the changes in solution pH and conductivity in the stabilization tank during the carbonation. The behavior of conductivity in the solution during the carbonation agrees well with those of a previous study, in which three different regions were observed in the conductivity graph [32].

The conductivity values of the solution at different carbonation conditions showed a linear decreasing trend, verifying the consumption of Ca^{2+} ions [33,39] due to their reaction with CO_2. The solution pH decreased slightly until the conductivity value decreased to almost zero (0.25 ± 0.01 μS/cm), indicating that PCC production has reached its

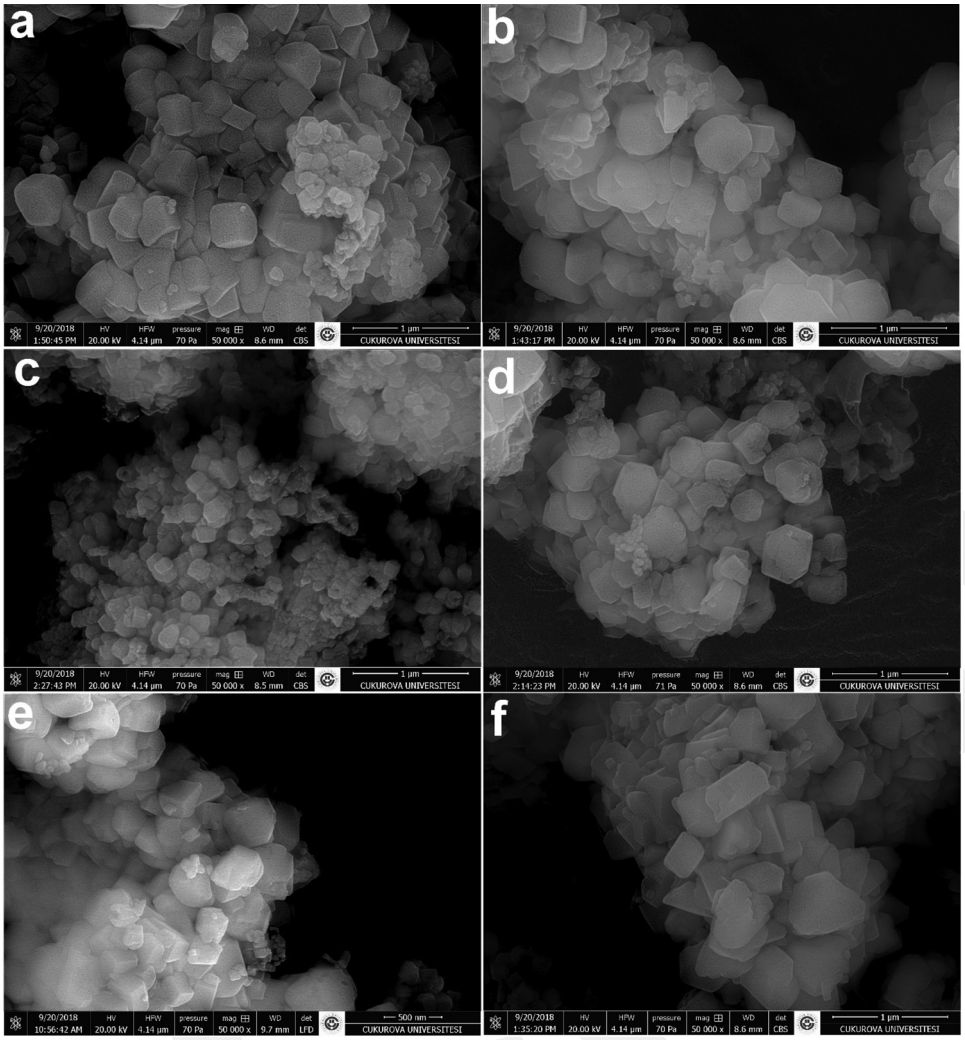

Fig. 5. SEM images of PCC produced at various experimental conditions: a) CF1R1V1, b) CF0.3R1V1, c) CF1R2V1, d) CF1R1V2, e) CF1R2V2, f) CF0.3R2V2.

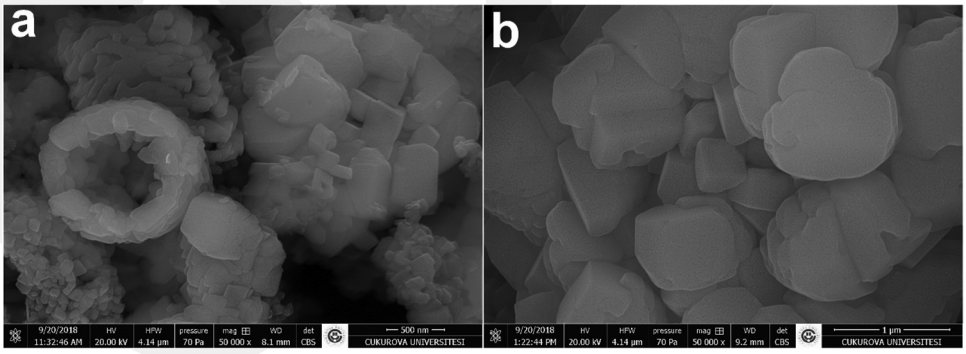

Fig. 6. SEM images of PCC produced at various experimental conditions: a) CF1RXVX b)CF0.3RXVX.

end point, while the solution pH was around 10, which is similar to that determined in a previous study [32]. These findings are in line with those of previous studies [41,42], which indicated that all Ca^{2+} ions in solution were totally carbonated as PCC before a hatched region in the pH graph where steep changes in pH occurred. Thereafter, a decreasing trend of the solution pH was observed.

The decrease in pH from around 12 to 7 was due to the absence of Ca^{2+} ions in the solution. Thus, the accumulation of H^+ and HCO_3^- ions made the solution acidic [33,42,43]. This resulted in the dissolution of Ca^{2+} ions from PCC particles, which is proved by the conductivity value of the solution that showed an increasing trend [33]. For this reason, the reaction was complete when the conductivity of the solution decreased to almost zero.

Ulkeryildiz et al. [33] indicated that the precipitation rate of PCC can be determined using Ca^{2+} ion, $Ca(OH)_2$, or CO_2 consumption rate according to the overall reaction for PCC production. In this study, we determined precipitation rate based on Ca^{2+} ion consumption, which can be predicted using the conductivity value of the solution. It was assumed that all Ca^{2+} ions were totally carbonated when the conductivity value was about 0.25 ± 0.01 μS/cm. The maximum precipitation rate of PCC in the absence of Venturi tube was calculated to be 32.43 μM/s, whereas when Venturi tubes were used, the reaction

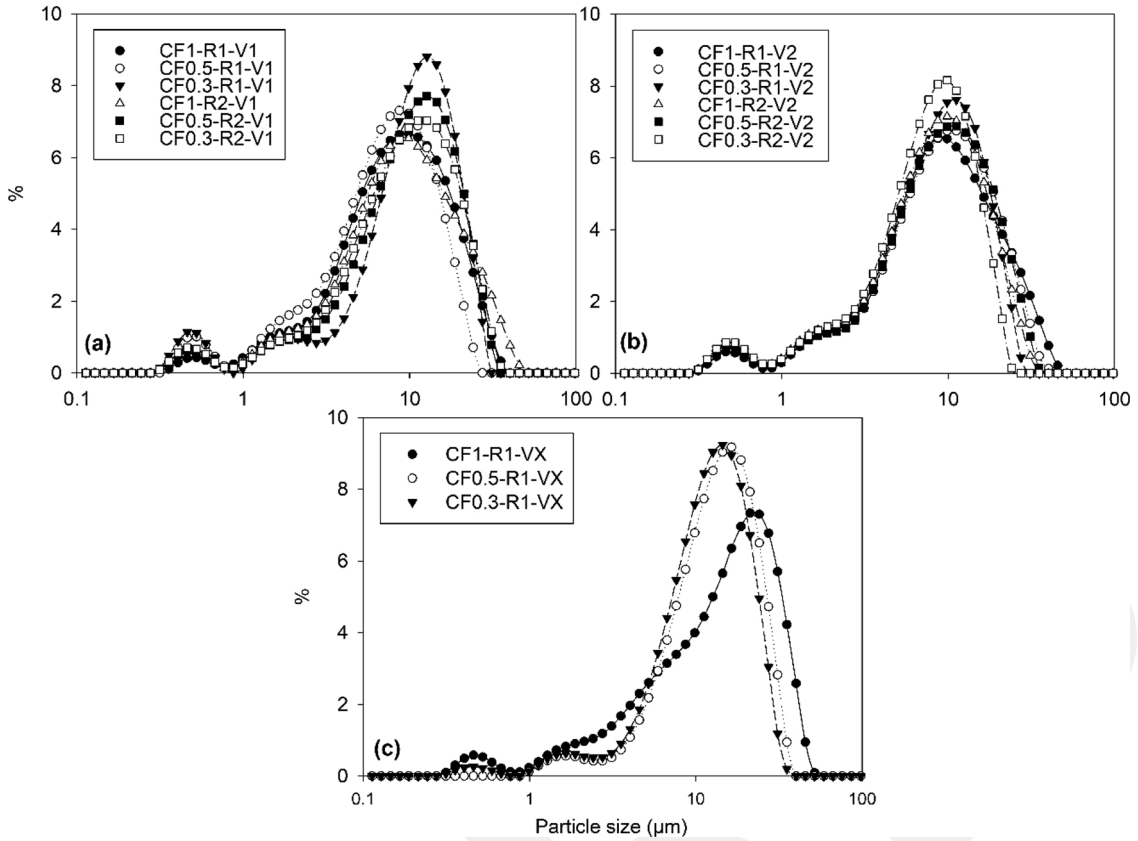

Fig. 7. Particle size distribution of produced $CaCO_3$ particles using (a) V1, (b) V2, and (c) VX.

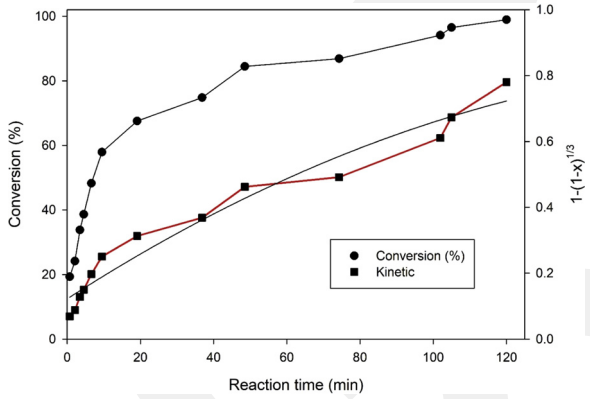

Fig. 8. Dissolution behavior of selected PCC particles versus time.

was completed in a shorter time because of higher reaction rates, as shown in Table 2.

The precipitation rate of PCC was found to be 30.77, 31.58, and 32.43 μM/s under the conditions of CF1-R1-V1, CF1-R1-V2, and CF1-RX-VX, respectively. At the CO_2 flow rate of 1 l/min, there was no remarkable change in the precipitation rate of PCC when Venturi tubes (V1 or V2) were used and when no Venturi tube was used (VX). When the CO_2 flow rate decreased from 1 l/min to 0.5 l/min, the precipitation rate of PCC using V1 and V2 decreased from 30.77 and 31.58 μM/s to 23.08 and 26.09 μM/s, respectively. These rates are 1.5 and 1.7 times higher than the precipitation rate of PCC for VX at the CO_2 flow rate of 0.5 l/min. This difference can be explained by the Reynolds number as follows: An increase in the Reynolds number of the solution led to an increase in the rate of mass transfer during the carbonation, and therefore, the reaction was completed in a shorter time. The effect of the circulation velocity on the precipitation rate of PCC is significant. For example, under CO_2 flow rate of 0.3 l/min and circulation velocity of 187.54 m/s (R_e: 69.96 × 10^4), CO_2 was produced in 740 s. However,

Table 3
Comparison of the reactivity value of selected PCC particles with a limestone used in previous studies.

Sample	Chemical Composition (%)						Reaction Rate Constant (min^{-1})
	$CaCO_3$	$MgCO_3$	Fe_2O_3	Al_2O_3	SiO_2	K_2O	
Yatagan Limestone [34]	95.29	1.72	0.38	0.75	1.54	0.12	24×10^{-4}
Yenikoy limestone [36]	97.10	0.41	0.37	0.61	1.29	0.08	29×10^{-4}
Kemerköy limestone [36]	98.45	0.37	0.38	0.14	0.54	0.02	31×10^{-4}
T-MW1 [36]	98.79	0.90	0.13	0.03	0.06	0.00	28×10^{-4}
T-MW2 [36]	87.70	10.15	1.42	0.22	0.42	0.01	19×10^{-4}
T-MW3 [36]	95.46	4.17	0.22	0.04	0.06	0.00	22×10^{-4}
Marble waste [37]	97.80	1.20	0.66	0.08	0.12	0.10	2.9×10^{-4}
This paper	99.63	ND	ND	0.26	ND	ND	52×10^{-4}

ND: not determined.

when the circulation velocity of the solution was 1167.63 m/s (R_e: 18.58×10^6), almost all Ca^{2+} ions transformed into PCC particles in 450 s. Significantly higher precipitation rates of PCC were realized using V2, compared to using V1, except for the carbonation test at the CO_2 flow rate of 1 l/min.

Researchers [32] found that in multiple experiments, CO_2 solubility remained constant when temperature and ion concentration were unchanged; hence, they pointed out that the time required for PCC production is highly dependent on the CO_2 flow rate. However, the experimental findings obtained in the present study are not consistent with those of the previous study [30]. When the V1, V2, and VX results were examined, it was obvious that the carbonation zone where Ca^{2+} ions and CO_2 gas reacted to produce PCC is important. Furthermore, the geometric property of the Venturi had a strong influence on the precipitation rate of PCC and led to an acceleration of the carbonation mechanism. Thus, PCC could be produced in a shorter time using Venturi tubes than without Venturi tube (VX).

Fig. 4 shows the XRD patterns of PCC produced under different experimental conditions. The major peaks observed at 29.41°, 47.50°, and 48.50° prove the production of calcite polymorph of $CaCO_3$ under all experimental conditions. Other peaks in the pattern correspond to calcite crystal, and no characteristic peaks representing portlandite mineral as an impurity were observed in the XRD pattern. This indicates the high quality of the PCC. However, the intensity of the major peak representing the calcite mineral differed. This is related to the experimental factors involved in the PCC production. Moreover, the use of Venturi in the carbonation process did not affect the crystallite size of the produced PCC, which varied between 31.99–58.01 nm; when no Venturi was used, the crystallite size of PCC was in a range of 35.01–40.21 nm. The crystallite size of PCC determined using the Scherrer equation can be seen in Table S1 in the Appendix.

Fig. 5(a)–(f) shows the SEM images of the PCC particles produced using V1 or V2. Clustered cubic crystals were observed in the SEM images. As understood from these SEM images, these observations agree with the XRD results, as PCC containing cubic shapes was identified as a typical calcite crystal; this was also observed in previous studies. [44,45]. However, the size of these crystals showed a difference depending on the circulation rate of the solution. An increase in the circulation rate of the solution resulted in the production of PCC that contained small cubic calcite crystals (Fig. 5c–e); these crystals are smaller than those obtained using lower circulation rates (Fig. 5a–d).

The SEM images given in Fig. 6(a)–(b) indicate that the PCC produced using VX did not have a uniform crystal structure, and a mixture of hollow spherical and cubic crystals was formed. In addition, the size of that crystals was higher than that of the PCC produced using V1 or V2. By comparing the SEM images of Figs. 5 and 6, it was found that the use of Venturi as the carbonation zone had a great influence on the crystal structure of PCC and resulted in producing PCC with a uniform crystal structure compared to the PCC obtained with no Venturi tube.

The SEM images reveal that larger polycrystalline PCC particles were formed as a result of the agglomeration of nano-sized cubic crystals, which are in line with the results obtained from the particle size analysis as shown in Fig. 7. Table S2 gives the parameters of the particle size distribution of each produced PCC particles. The d_{50} value of the PCC produced using V1 or V2 varied between 7.66 and 11.20 μm, whereas the d_{50} value of the PCC produced using VX was higher than 13 μm. However, each produced PCC showed a similar monomodal pattern. The SPAN factor given in Table S2 indicates that although PCC with a higher particle size was produced using VX, its distribution was narrower than the PCC obtained using V1 and V2.

3.3. Reactivity test

Researchers have indicated that the reactivity property of solid particles is one of the important parameters for the desulfurization unit design [46]. Therefore, a reactivity test was performed on the PCC particles produced at the condition of CF1-V2-R2 to evaluate the use of PCC in the desulfurization unit. Fig. 8 shows the dissolution behavior of selected PCC particles.

At the 15th min, the conversion ratio of the PCC reached 70%, which is somewhat higher than those of previous studies [36,37]. Depending on time, almost all PCC particles dissolved in the presence of HCl acid at the 100th min. This difference is related to the chemical composition of the sorbent, which has been explained in detail in a previous study [36]. An increase in the purity of the sorbent in terms of its constituent calcite crystals led to an increase in the dissolution rate of the sorbent. The PCC particles produced herein was mainly composed of Ca, C, and O elements, and no impurities were observed, according to the EDS spectrum given in Fig. S1. The reaction rate constant of the PCC was $52 \times 10^{-4}\,min^{-1}$, which is rather higher than those of previous studies, as shown in Table 3.

4. Conclusion

This study focused on the production of PCC particles from DG using a developed experimental apparatus that comprised of carbonation and stabilization zones. A Venturi tube was used as the carbonation zone, in which CO_2 gas and solution were mixed to produce PCC particles. The PCC particles produced herein were characterized by XRD, SEM, and particle size analyses. The experimental results indicate that the required reaction time for producing PCC particles using the Venturi tube was up to two times lower than that without using Venturi tube. All produced PCC particles were identified as calcite mineral. However, their crystal structure properties were influenced by the experimental conditions. The PCC particles produced using V1 or V2 were composed of uniform clustered nano-sized cubic crystals, while a mixture of spherical and cubic crystals was formed with no Venturi tube (VX).

The main advantages for the use of Venturi tube as the carbonation zone compared to the control experiments are summarized as follows: (i) PCC was obtained in a shorter time with an increase in the circulation rate of the solution, (ii) the precipitation rate of PCC was higher, and (iii) PCC with nano-sized cubic crystals was produced. However, the main disadvantage for the use of Venturi tube is that agglomerated PCC particles were obtained. This problem may be solved by using ultrasonic treatment or some chemicals. In addition, sodium sulfate was obtained as a co-product, which can be evaluated in the chemical industry (detergent or paper industries) [26].

Furthermore, the reactivity of the produced PCC particles indicated that the use of PCC in the desulfurization unit yielded satisfactory results compared to those of previous studies in which limestone or marble waste was used as a sorbent. There was no need to conduct any mineral processing operations (crushing and grinding); however, limestone and marble waste must be pulverized by these operations to obtain a sorbent of below 45 μm before being used in a desulfurization unit. The evaluation of PCC obtained from gypsum wastes in more profitable industrial areas such as paper, plastics or food industry will be investigated in future studies.

Acknowledgment

This study was supported by Çukurova University [Project ID: FBA-2017-7912].

Appendix A. Supplementary data

Supplementary material related to this article can be found, in the online version, at doi:https://doi.org/10.1016/j.jcou.2018.12.004.

References

[1] H. Tayibi, M. Choura, F.A. López, F.J. Alguacil, A. López-Delgado, Environmental impact and management of phosphogypsum, J. Environ. Manage. 90 (2009)

2377–2386.
[2] I. Fauziah, S. Zauyah, T. Jamal, Characterization and land application of red gypsum: a waste product from the titanium dioxide industry, Sci. Total Environ. 188 (1996) 243–251.
[3] J. Kang, X. Gou, Y. Hu, W. Sun, R. Liu, Z. Gao, Q. Guan, Efficient utilisation of flue gas desulfurization gypsum as a potential material for fluoride removal, Sci. Total Environ. 649 (2018) 344–352.
[4] R.B. Bryant, A.R. Buda, P.J. Kleinman, C.D. Church, L.S. Saporito, G.J. Folmar, S. Bose, A.L. Allen, Using flue gas desulfurization gypsum to remove dissolved phosphorus from agricultural drainage waters, J. Environ. Qual. 41 (2012) 664–671.
[5] T. DeSutter, L. Cihacek, Potential agricultural uses of flue gas desulfurization gypsum in the northern Great Plains, Agron. J. 101 (2009) 817–825.
[6] C. Leiva, C.G. Arenas, L. Vilches, J. Vale, A. Gimenez, J. Ballesteros, C. Fernández-Pereira, Use of FGD gypsum in fire resistant panels, Waste Manag. 30 (2010) 1123–1129.
[7] A. Telesca, M. Marroccoli, D. Calabrese, G.L. Valenti, F. Montagnaro, Flue gas desulfurization gypsum and coal fly ash as basic components of prefabricated building materials, Waste Manag. 33 (2013) 628–633.
[8] B. Ma, X. Li, Y. Mao, X. Shen, Synthesis and characterization of high belite sulfoaluminate cement through rich alumina fly ash and desulfurization gypsum, Ceram. Silik 57 (2013) 7–13.
[9] W. Wang, X. Wang, J. Zhu, P. Wang, C. Ma, Experimental investigation and modeling of sulfoaluminate cement preparation using desulfurization gypsum and red mud, Ind. Eng. Chem. Res. 52 (2013) 1261–1266.
[10] K. Song, Y.-N. Jang, W. Kim, M.G. Lee, D. Shin, J.-H. Bang, C.W. Jeon, S.C. Chae, Precipitation of calcium carbonate during direct aqueous carbonation of flue gas desulfurization gypsum, Chem. Eng. J. 213 (2012) 251–258.
[11] J. Zhao, X. Song, Z. Sun, Y. Xu, J. Yu, Design and optimization of the preparation of calcium carbonate from calcium sulfate and ammonium bicarbonate, Int. J. Chem. React. Eng. 12 (2014).
[12] A. Azdarpour, M. Asadullah, E. Mohammadian, R. Junin, H. Hamidi, M. Manan, A.R.M. Daud, Mineral carbonation of red gypsum via pH-swing process: Effect of CO2 pressure on the efficiency and products characteristics, Chem. Eng. J. 264 (2015) 425–436.
[13] W. Ding, H. Yang, J. Ouyang, Mineral carbonation of a desulfurization residue for CO2 sequestration, RSC Adv. 5 (2015) 67184–67194.
[14] H.-P. Mattila, R. Zevenhoven, Mineral carbonation of phosphogypsum waste for production of useful carbonate and sulfate salts, Front. Energy Res. 3 (2015).
[15] S.M. Pérez-Moreno, M.J. Gázquez, J.P. Bolívar, CO 2 sequestration by indirect carbonation of artificial gypsum generated in the manufacture of titanium dioxide pigments, Chem. Eng. J. 262 (2015) 737–746.
[16] K. Song, W. Kim, J.-H. Bang, S. Park, C.W. Jeon, Polymorphs of pure calcium carbonate prepared by the mineral carbonation of flue gas desulfurization gypsum, Mater. Des. 83 (2015) 308–313.
[17] H. Cheng, X. Wang, B. Wang, J. Zhao, Y. Liu, F. Cheng, Effect of ultrasound on the morphology of the CaCO3 precipitated from CaSO4-NH3-CO2-H2O system, J. Cryst. Growth (2016).
[18] S.Q. Lu, P.Q. Lan, S.F. Wu, Preparation of Nano-CaCO3 from phosphogypsum by gas–Liquid–Solid reaction for CO2 sorption, Ind. Eng. Chem. Res. 55 (2016) 10172–10177.
[19] O. Rahmani, A. Kadkhodaie, J. Highfield, Kinetics analysis of CO2 mineral carbonation using byproduct red gypsum, Energy Fuels 30 (2016) 7460–7464.
[20] K. Song, W. Kim, S. Park, J.-H. Bang, C.W. Jeon, J.-W. Ahn, Effect of polyacrylic acid on direct aqueous mineral carbonation of flue gas desulfurization gypsum, Chem. Eng. J. 301 (2016) 51–57.
[21] H. Xie, J. Wang, Z. Hou, Y. Wang, T. Liu, L. Tang, W. Jiang, CO2 sequestration through mineral carbonation of waste phosphogypsum using the technique of membrane electrolysis, Environ. Earth Sci. 75 (2016).
[22] A. Azdarpour, M. Afkhami Karaei, H. Hamidi, E. Mohammadian, B. Honarvar, CO 2 sequestration through direct aqueous mineral carbonation of red gypsum, Petroleum (2017).
[23] W. Bao, H. Zhao, H. Li, S. Li, W. Lin, Process simulation of mineral carbonation of phosphogypsum with ammonia under increased CO 2 pressure, J. Co2 Util. 17 (2017) 125–136.
[24] S. De Gisi, A. Molino, M. Notarnicola, Enhancing the recovery of gypsum in limestone-based wet flue gas desulfurization with high energy ball milling process: a feasibility study, Process. Saf. Environ. Prot. 109 (2017) 117–129.
[25] O. Rahmani, CO2 sequestration by indirect mineral carbonation of industrial waste red gypsum, J. Co2 Util. 27 (2018) 374–380.
[26] C. Cardenas-Escudero, V. Morales-Florez, R. Perez-Lopez, A. Santos, L. Esquivias, Procedure to use phosphogypsum industrial waste for mineral CO_2 sequestration, J. Hazard. Mater. 196 (2011) 431–435.
[27] Y. N. Jang, W. R. Kyung, K. L. Myung, Production method for high-purity calcite and ammonium sulphate by using gypsum, U.S. Patent No. WO2013/012214.
[28] M. Altiner, Effect of alkaline types on the production of calcium carbonate particles from gypsum waste for fixation of CO2 by mineral carbonation, Int. J. Coal Prep. Util. (2018) 1–19.
[29] O. Rahmani, Siderite precipitation using by-product red gypsum for CO 2 sequestration, J. Co2 Util. 24 (2018) 321–327.
[30] H. Casanova, L.P. Higuita, Synthesis of calcium carbonate nanoparticles by reactive precipitation using a high pressure jet homogenizer, Chem. Eng. J. 175 (2011) 569–578.
[31] C.R. Blue, A. Giuffre, S. Mergelsberg, N. Han, J.J. De Yoreo, P.M. Dove, Chemical and physical controls on the transformation of amorphous calcium carbonate into crystalline CaCO 3 polymorphs, Geochim. Cosmochim. Acta 196 (2017) 179–196.
[32] D. Konopacka-Łyskawa, Z. Cisiak, B. Kawalec-Pietrenko, Effect of liquid circulation in the draft-tube reactor on precipitation of calcium carbonate via carbonation, Powder Technol. 190 (2009) 319–323.
[33] E. Ulkeryildiz, S. Kilic, E. Ozdemir, Nano-CaCO 3 synthesis by jet flow, Colloids Surf. A: Physicochem. Eng. Aspects 512 (2017) 34–40.
[34] F.F. Peng, X. Yu, Pico–nano bubble column flotation using static mixer-venturi tube for Pittsburgh No. 8 coal seam, Int. J. Min. Sci. Technol. 25 (2015) 347–354.
[35] P. Scherrer, Determination of the size and internal structure of colloidal particles using X-rays, Nachr. Ges. Wiss. Göttingen 2 (1918) 98–100.
[36] N.E. Altun, Assessment of marble waste utilization as an alternative sorbent to limestone for SO 2 control, Fuel Process. Technol. 128 (2014) 461–470.
[37] N.E. Altun, Reactivity of marble wastes for potential utilization in wet flue gas desulphurization, Physicochem. Probl. Miner. Process. 52 (2016) 497–509.
[38] C.D. Blasio, E. Mäkilä, T. Westerlund, Use of carbonate rocks for flue gas desulfurization: reactive dissolution of limestone particles, Appl. Energy 90 (2012) 175–181.
[39] S. Kilic, G. Toprak, E. Ozdemir, Stability of CaCO3 in Ca(OH)2 solution, Int. J. Miner. Process. 147 (2016) 1–9.
[40] E. Chibowski, L. Hołysz, A. Szcześ, M. Chibowski, Precipitation of calcium carbonate from magnetically treated sodium carbonate solution, Colloids Surf. A: Physicochem. Eng. Aspects 225 (2003) 63–73.
[41] J.-H. Bang, Y.N. Jang, W. Kim, K.S. Song, C.W. Jeon, S.C. Chae, S.-W. Lee, S.-J. Park, M.G. Lee, Precipitation of calcium carbonate by carbon dioxide microbubbles, Chem. Eng. J. 174 (2011) 413–420.
[42] M. Altiner, Influences of CO2 bubbling types on preparation of calcite nanoparticles by carbonation process, Period. Polytech. Chem. Eng. 62 (2018) 209–214.
[43] L. Xiang, Y. Xiang, Y. Wen, F. Wei, Formation of CaCO3 nanoparticles in the presence of terpineol, Mater. Lett. 58 (2004) 959–965.
[44] Y. Ding, Y. Liu, Y. Ren, H. Yan, M. Wang, D. Wang, X.-Y. Lu, B. Wang, T. Fan, H. Guo, Controllable synthesis of all the anhydrous CaCO3 polymorphs with various morphologies in CaCl2-NH3-CO2 aqueous system, Powder Technol. 333 (2018) 410–420.
[45] J. Yu, M. Lei, B. Cheng, X. Zhao, Effects of PAA additive and temperature on morphology of calcium carbonate particles, J. Solid State Chem. 177 (2004) 681–689.
[46] Z. Shen, X. Chen, M. Tong, S. Guo, M. Ni, J. Lu, Studies on magnesium-based wet flue gas desulfurization process with oxidation inhibition of the byproduct, Fuel 105 (2013) 578–584.